

1.00000  
707

## TURBULENCE MODELING AND COMPUTATION OF TURBINE AERODYNAMICS AND HEAT TRANSFER

B. Lakshminarayana & J. Luo  
The Pennsylvania State University  
Center for Gas Turbine & Power  
University Park, PA 16802

The objective of the present research is to develop improved turbulence models for the computation of complex flows through turbomachinery passages, including the effects of streamline curvature, heat transfer and secondary flows.

Advanced turbulence models are crucial for accurate prediction of rocket engine flows, due to existence of very large extra strain rates, such as strong streamline curvature. Numerical simulation of the turbulent flows in strongly curved ducts, including two 180-deg ducts, one 90-deg duct and a strongly concave curved turbulent boundary layer have been carried out with Reynolds stress models (RSM) and algebraic Reynolds stress models (ARSM). The RSM & ARSM models are successful in the prediction of damping effects of convex curvature. However, both models underpredict the turbulence amplification caused by strong concave curvature. In order to capture this amplification of turbulence, the time scale (for spectral energy transfer) in the dissipation rate ( $\epsilon$ ) equation must be modified. A detailed analysis has been carried out for the modifications to the  $\epsilon$ -equation. An improved near-wall pressure-strain correlation has been developed for capturing the anisotropy of turbulence in the concave region.

A comparative study of two modes of transition in gas turbine, the by-pass transition and the separation-induced transition, has been carried out with several representative low-Reynolds-number (LRN)  $k$ - $\epsilon$  models. Effects of blade surface pressure gradient, freestream turbulence and Reynolds number on the blade boundary layer development, and particularly the inception of transition are examined in detail. The present study indicates that the turbine blade transition, in the presence of high freestream turbulence, is predicted well with LRN  $k$ - $\epsilon$  models employed.

The three-dimensional Navier-Stokes procedure developed by the present authors has been used to compute the three-dimensional viscous flow through the turbine nozzle passage of a single stage turbine. A low Reynolds number  $k$ - $\epsilon$  model and a zonal  $k$ - $\epsilon$ /ARSM (algebraic Reynolds stress model) are utilized for turbulence closure. The algebraic Reynolds stress model is used only in the endwall region to represent the anisotropy of turbulence. For the turbine nozzle flow, comprehensive comparisons between the predictions and the experimental data obtained at Penn State show that most features of the vortex-dominated endwall flow, as well as nozzle wake structure, have been captured well by the numerical procedure. An assessment of the performance of the turbulence models has been carried out. The two models are found to provide similar predictions for the mean flow parameters, although slight improvement in the prediction of some secondary flow quantities has been obtained by the ARSM model. It's found that the wake profiles inside the endwall boundary layers are predicted better than those near the mid-span.

**TURBULENCE MODELING AND COMPUTATION OF TURBINE  
AERODYNAMICS AND HEAT TRANSFER\***

**B. Lakshminarayana and J. Luo**

**Center for Gas Turbine & Power  
The Pennsylvania State University  
University Park, PA 16802**

**CFD Workshop, April 25, 1995, Huntsville, AL**

**\* Sponsored by NASA Marshall Space Flight Center**

## **Objective:**

**To develop turbulence models for prediction of turbine flow & thermal fields including effects of curvature, rotation and high temperature**

## **Outline:**

429

- **Introduction**
- **Numerical Technique & Turbulence Models**
- **3-D Navier-Stokes Comp. of turbine nozzle flow**
- **Turbulence Modeling for Strongly Curved Shear Flows**
- **Computation of Turbine Blade Transition and Heat Transfer**
- **Concluding remarks**

## 3-D NAVIER-STOKES PROCEDURE

- **Explicit 4-Stage Runge-Kutta Scheme**
- **Central differencing + smoothing (eigenvalue & local vel. scaling)**
- **Turbulence Models:**
  - **Differential Reynolds stress model (high Re no. & low Re no.)**
  - **Algebraic Reynolds stress model**
  - **Nonlinear k- $\epsilon$  model**
  - **Two eq. models (low & high-Re-no. versions)**
  - **$\epsilon$ -modification for strong streamline curvature**
- **Boundary Conditions**
  - **Characteristic boundary conditions**
  - **Quasi-3D non-reflecting boundary conditions**
- **Acceleration Schemes**
  - **Local time stepping, implicit residual smoothing**
  - **Implicit treatment of k- $\epsilon$  equations**
  - **Multigrid**

Strongly curved shear flows investigated:

Flow	Author	Re	$\delta/R$
<u>Concave TBL</u>	<u>Barlow &amp; Johnston</u>	<u><math>3.3 \times 10^4</math></u>	<u>0.06</u>
<u>90-deg duct</u>	<u>Kim &amp; Patel</u>	<u><math>2.2 \times 10^5</math></u>	<u>0.05/0.04</u>
<u>180-deg duct</u>	<u>Monson et al.</u>	<u><math>1.0 \times 10^5</math></u>	<u>0.7/0.2</u>
<u>180-deg duct</u>	<u>Sandborn</u>	<u><math>2.2 \times 10^5</math></u>	<u>1.0/0.3</u>
<u>180-deg duct</u>	<u>Monson et al.</u>	<u><math>1.0 \times 10^6</math></u>	<u>0.7/0.2</u>

## Modeling for Curved Shear Flows

- Modeling of curved flows (mostly mild curvature, convex curvature)
  - Mixing-length model: Prandtl's hypothesis  $F = 1 - \alpha \frac{U/r}{\partial U / \partial n}$
  - k- $\epsilon$  model: Launder et al (1977)  $-C_{\epsilon 2} (1 - C_c Ri_t) \frac{\epsilon^2}{k}$ , etc.
  - RSM & ARSM: Irvin & Arnot Smith 1975, Gibson & Rodi 1981, etc.  
(used in boundary layer codes, mild/convex curved flows)

- Comps. of strongly curved flows, e.g., 180-deg duct flows.
  - Monson et al. (1990);
  - Avva et al. (1990);
  - Shih et al. (1994), etc.

**Agreement not satisfactory**

**=> Further modeling work on strongly curved flows**

## Modifications to $\varepsilon$ -equation

- **Standard  $\varepsilon$  equation:**

$$\frac{\partial(\rho\varepsilon)}{\partial t} + \frac{\partial(\rho U_i \varepsilon)}{\partial x_i} = \frac{\partial}{\partial x_j} \left[ \left( \mu + \frac{\mu_t}{\sigma_\varepsilon} \right) \frac{\partial \varepsilon}{\partial x_j} \right] + \rho \frac{\varepsilon}{k} (C_{\varepsilon 1} P_k - C_{\varepsilon 2} \varepsilon)$$

**standard values:  $C_\mu=0.09$ ,  $C_{\varepsilon 1}=1.44$ ,  $C_{\varepsilon 2}=1.92$ ,  $\sigma_k=1.0$ ,  $\sigma_\varepsilon=1.3$**

- **Modification in the sink term (Launder et al. 1977)**

$$C_{\varepsilon 2} = C_{\varepsilon 2} (1 - 0.2 Ri_t)$$

**where**  $Ri_t = \left( \frac{k}{\varepsilon} \right)^2 \frac{U}{r^2} \frac{\partial(Ur)}{\partial n}$

- **Modification of time-scale in the source term (Lumley 1992)**

$$\frac{\partial(\rho\varepsilon)}{\partial t} + \frac{\partial(\rho U_i \varepsilon)}{\partial x_i} = \frac{\partial}{\partial x_j} \left[ \left( \mu + \frac{\mu_t}{\sigma_\varepsilon} \right) \frac{\partial \varepsilon}{\partial x_j} \right] + \rho \frac{\varepsilon}{k} (C'_{\varepsilon 1} kS - C_{\varepsilon 2} \varepsilon)$$

**where**  $C'_{\varepsilon 1} = 0.42$ ,  $S = (2S_{ij}S_{ij})^{1/2}$ ,  $S_{ij} = (U_{i,j} + U_{j,i})/2$

**Nonlinear k-ε model (Shih, Zhu & Lumley 1993)**

$$\begin{aligned} \overline{u_i u_j} = & \frac{2}{3} k \delta_{ij} - v_t (U_{i,j} + U_{j,i}) \\ & + \frac{C_{\tau 1}}{A_2 + \eta^3} \frac{k^3}{\varepsilon^2} (U_{i,k} U_{k,j} + U_{j,k} U_{k,i} - \frac{2}{3} U_{i,j} U_{j,i} \delta_{ij}) \\ & + \frac{C_{\tau 2}}{A_2 + \eta^3} \frac{k^3}{\varepsilon^2} (U_{i,k} U_{j,k} - \frac{1}{3} U_{i,j} U_{i,j} \delta_{ij}) \\ & + \frac{C_{\tau 3}}{A_2 + \eta^3} \frac{k^3}{\varepsilon^2} (U_{k,i} U_{k,j} - \frac{1}{3} U_{i,j} U_{i,j} \delta_{ij}) \end{aligned}$$

434

$$v_t = \frac{2/3 k^2}{A_1 + \eta \varepsilon}$$

$$\eta = \frac{k}{\varepsilon} (2 S_{ij} S_{ij})^{1/2}$$

$$S_{ij} = (U_{i,j} + U_{j,i}) / 2$$



# ARSM (ALGEBRAIC REYNOLDS STRESS MODELS)

- Reynolds stress transport eq.:

$$C_{ij} - D_{ij} = P_{ij} + \phi_{ij} - \varepsilon_{ij}$$

- ARSM assumption (Rodi, 1976):

$$C_{ij} - D_{ij} = \frac{\overline{u_i u_j}}{k} (C_k - D_k) = \frac{\overline{u_i u_j}}{k} (P_k - \varepsilon)$$

- Present ARSM (Derived from Gibson & Launder RSM (1978) for compressible flows)

$$-\overline{\rho u_i'' u_j''} = -\bar{\rho} \bar{k} \left[ (P_{ij} - 2P\delta_{ij}/3)(1 - C_2) + \phi_{ij,w} \right] / \left[ P + \bar{\rho} \bar{\varepsilon} (C_1 - 1) \right] - \frac{2}{3} \delta_{ij} \bar{\rho} \bar{k}$$

$$P_{ij} = -\overline{\rho u_i'' u_k''} \partial \bar{u}_j / \partial x_k - \overline{\rho u_j'' u_k''} \partial \bar{u}_i / \partial x_k \quad \text{and} \quad P = P_{ii} / 2$$

## Low Reynolds-number RSM Models

### Shima, 1988

- Based on LRR RSM
- conventional damping function  $f_w$  ( $f_w = \exp(-(0.015k^{1/2}y/n)^4)$ )
- This LRN model reduces to its high-Re version (i.e., LRR model) away from the wall.

### Launder & Shima, 1989

- 436
- Based on LRR-Gibson-Launder RSM
  - Use independent Reynolds stress invariants
  - Constants  $C_1$ ,  $C_2$ ,  $C'_1$  and  $C'_2$  are functions of the turbulence anisotropy parameters
  - This model may not reduce to its high Re version away from the wall

## REYNOLDS-STRESS MODEL (RSM) AND ALGEBRAIC REYNOLDS-STRESS MODEL (ARSM)

- Reynolds stress transport equation :

$$U_k \frac{\partial \overline{u_i u_j}}{\partial x_k} = -\overline{u_i u_k} U_{j,k} - \overline{u_j u_k} U_{i,k} + \overline{\frac{p}{\rho} (u_{i,j} + u_{j,i})} - \frac{\partial}{\partial x_k} \left[ \overline{u_i u_j u_k} + \frac{\overline{p u_j}}{\rho} \delta_{ik} + \frac{\overline{p u_i}}{\rho} \delta_{jk} - \nu \frac{\partial \overline{u_i u_j}}{\partial x_k} \right] - 2\nu \frac{\partial \overline{u_i}}{\partial x_k} \frac{\partial \overline{u_j}}{\partial x_k}$$

437 i.e.,  $C_{ij} - D_{ij} = P_{ij} + \phi_{ij} - \epsilon_{ij}$

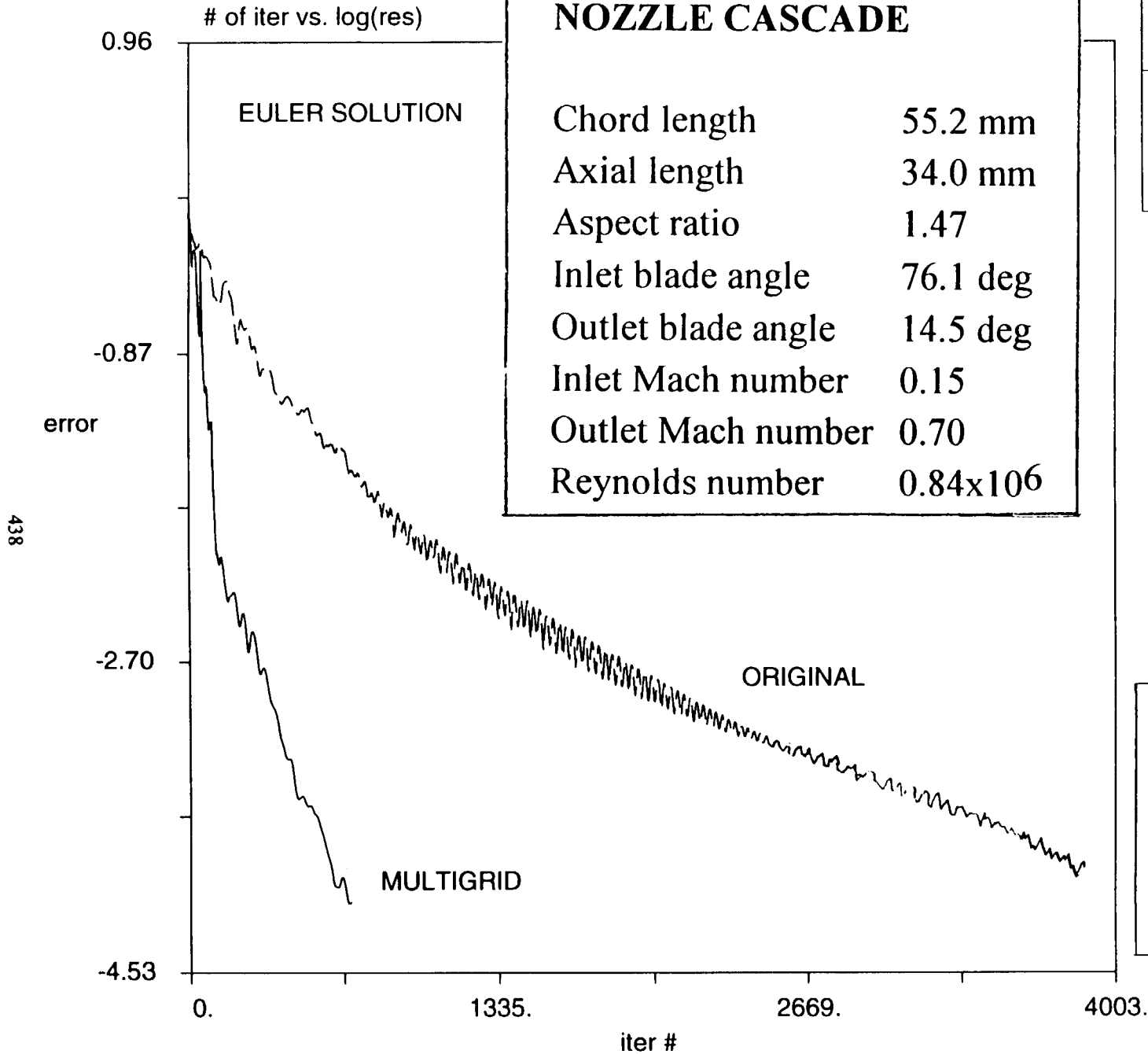
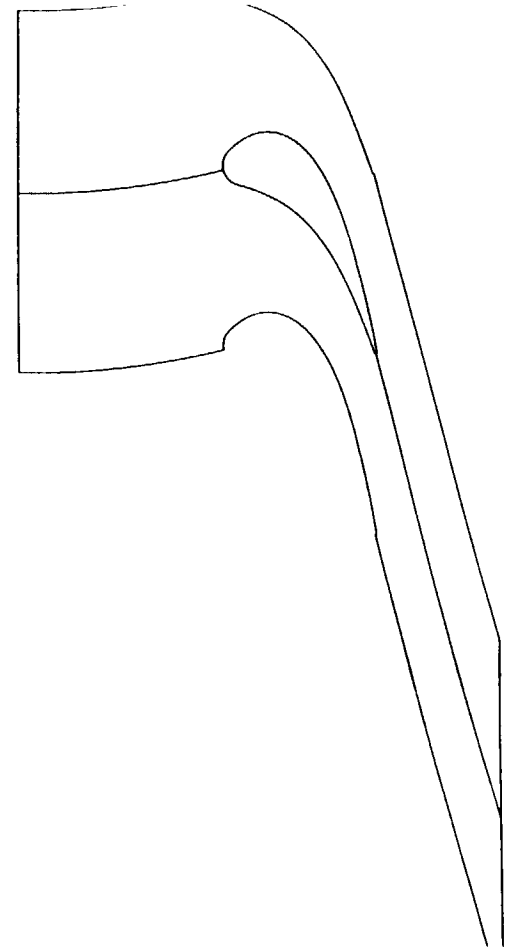
- Models employed in present computations:

- RSM model = LRR Model (Launder, Reece & Rodi, 1975)  
with Shima near-wall low-Reynolds-number functions

- ARSM model = Algebraic form of LRR model with Gibson-Launder near-wall Pressure-strain correlation

# PERDICHIZZI TURBINE NOZZLE CASCADE

Chord length	55.2 mm
Axial length	34.0 mm
Aspect ratio	1.47
Inlet blade angle	76.1 deg
Outlet blade angle	14.5 deg
Inlet Mach number	0.15
Outlet Mach number	0.70
Reynolds number	$0.84 \times 10^6$

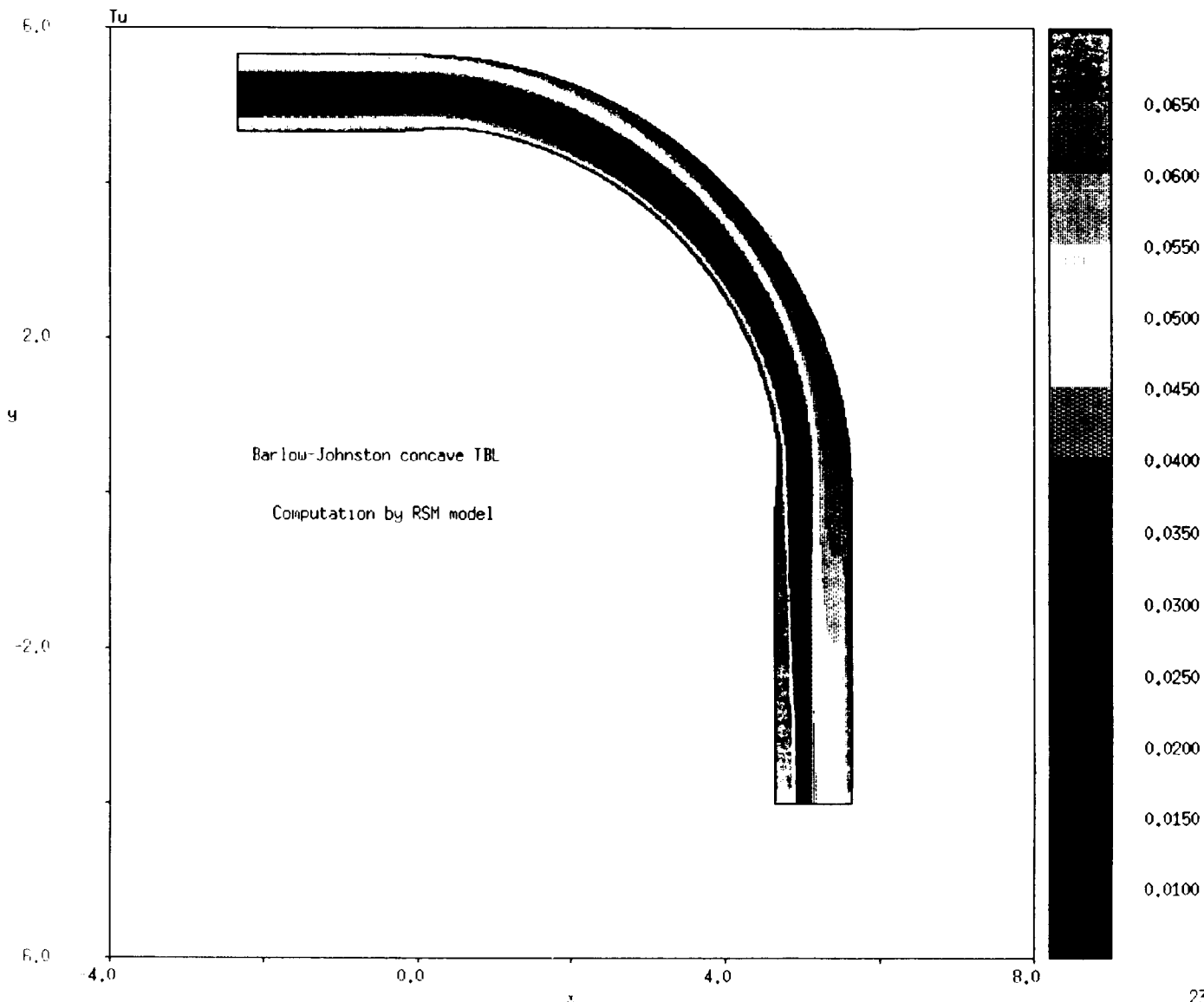


## IMPROVEMENT

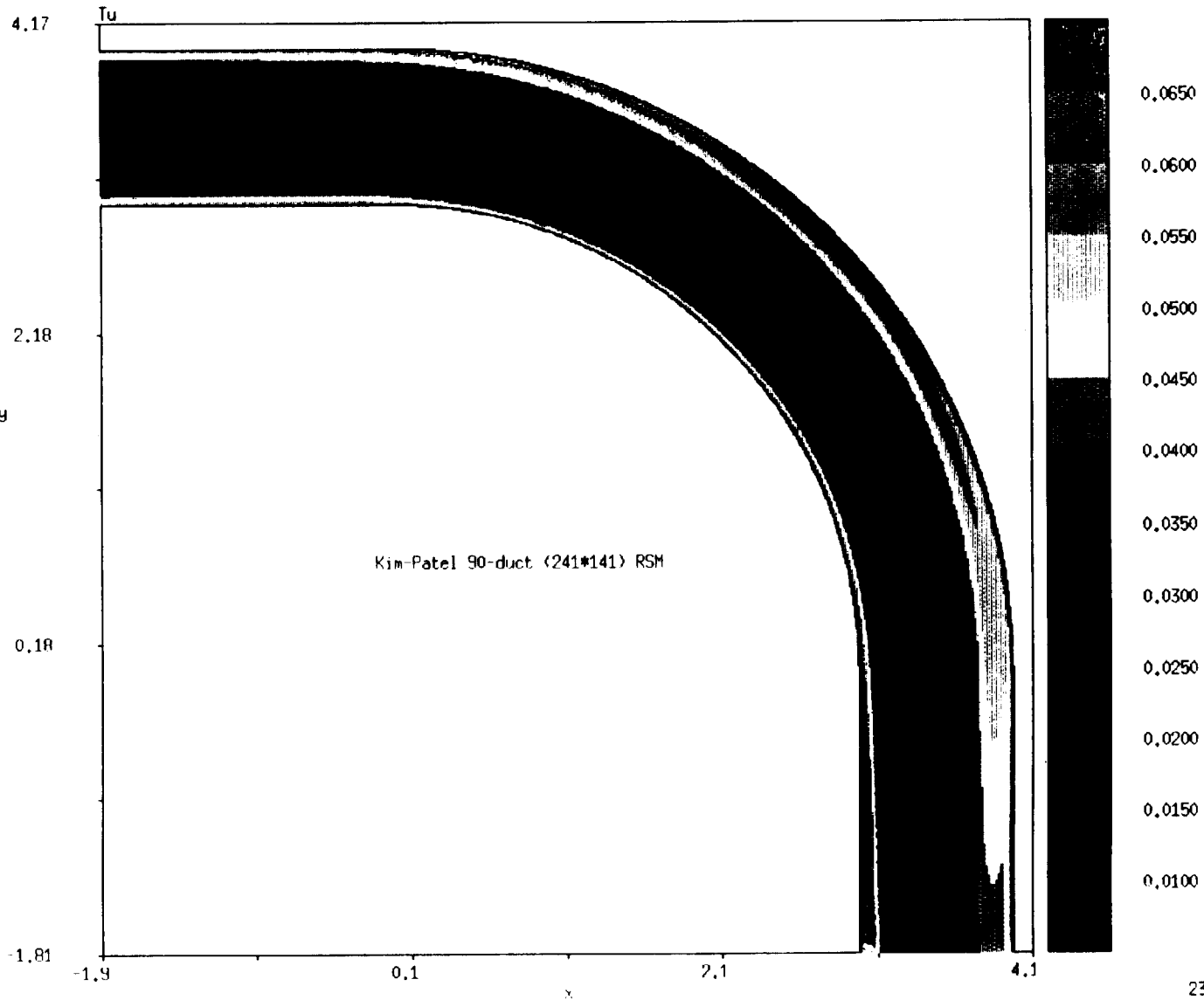
**5 : 1 Convergence Rate**

**4.3 : 1 CPU Time**

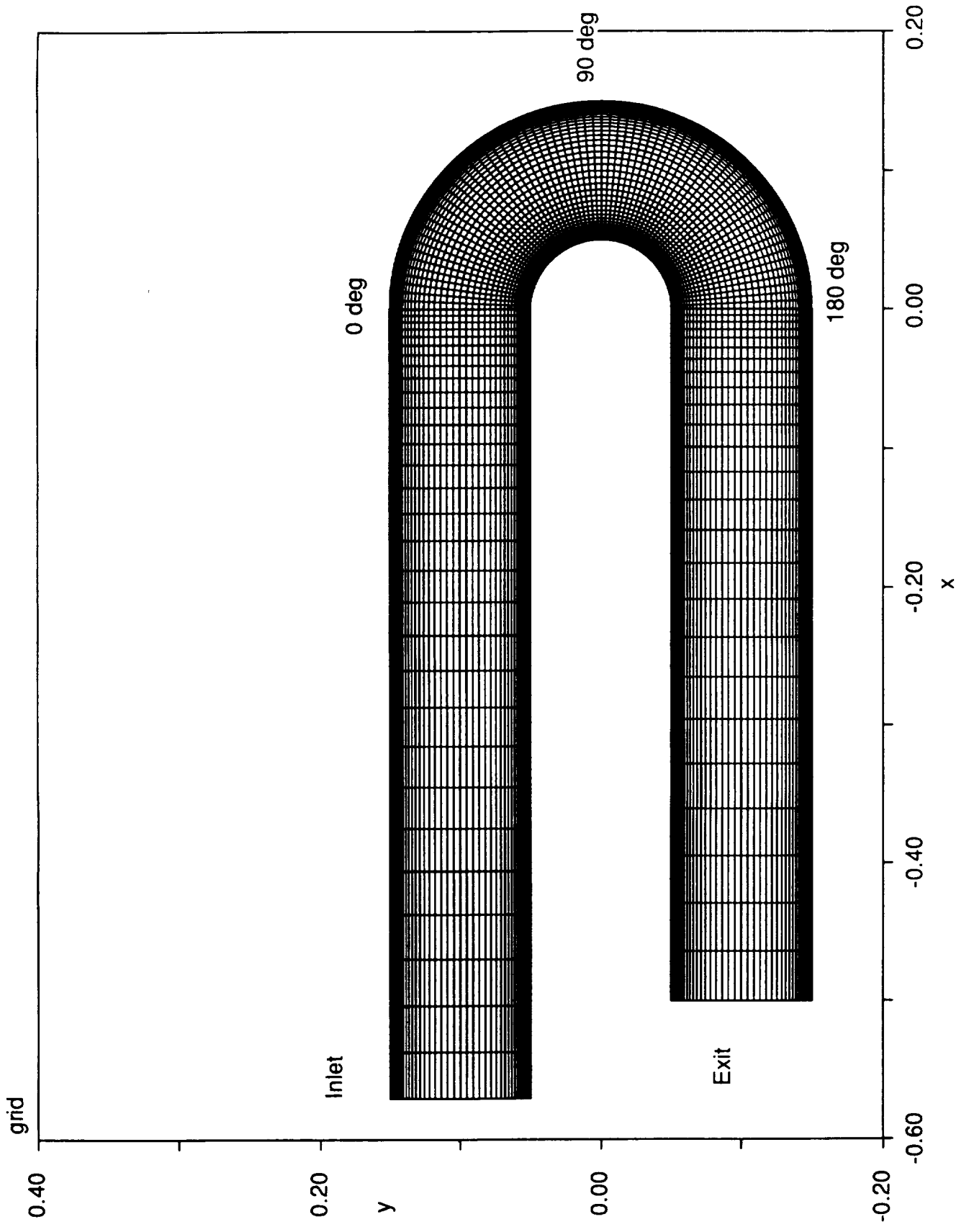
24 Apr 95 11:34:01



440



23 Apr 95 19:55:08



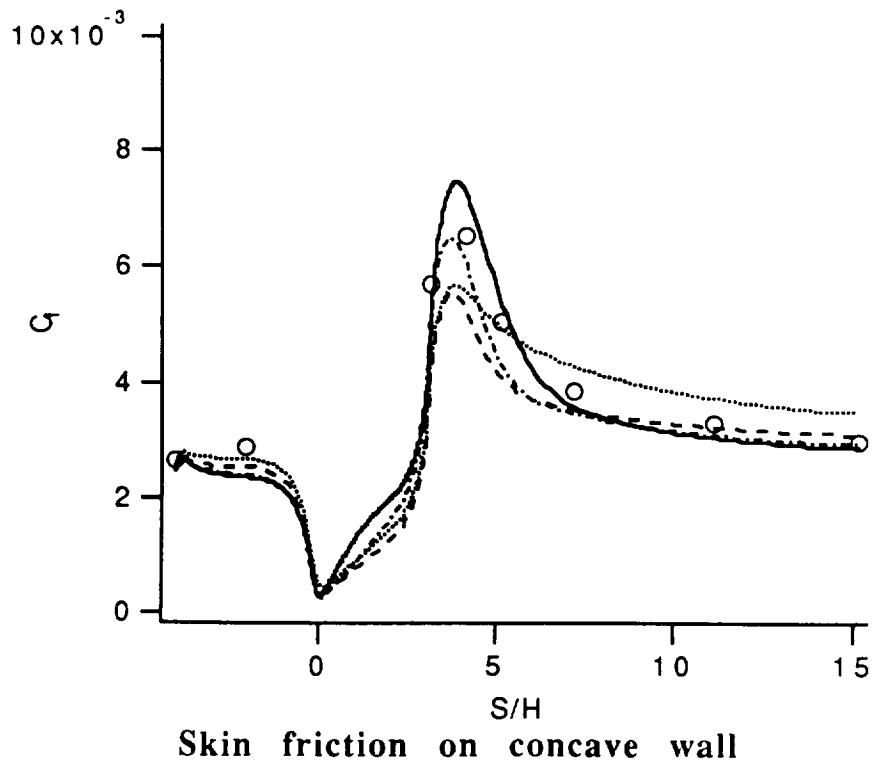
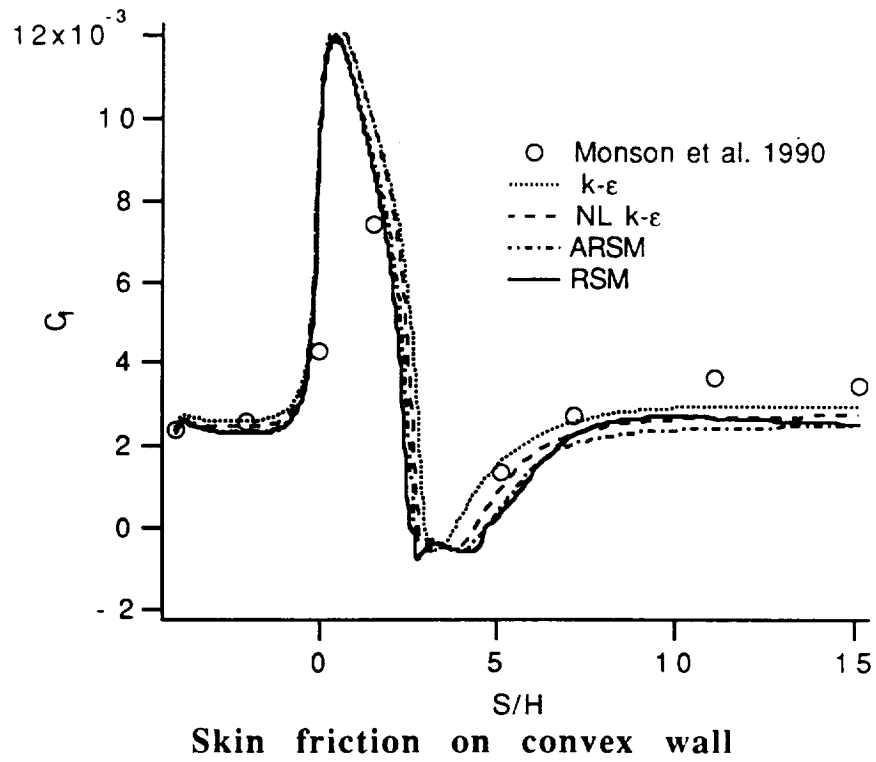
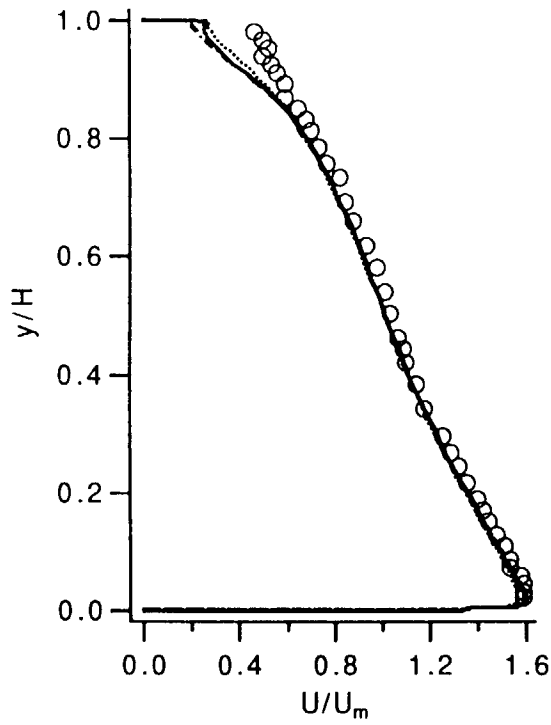
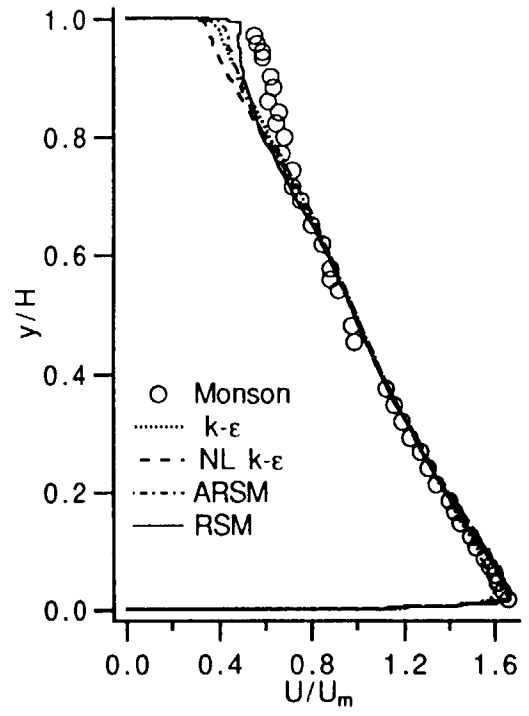


**Fig. Skin friction for Monson et al. ( $Re=1 \times 10^6$ )**

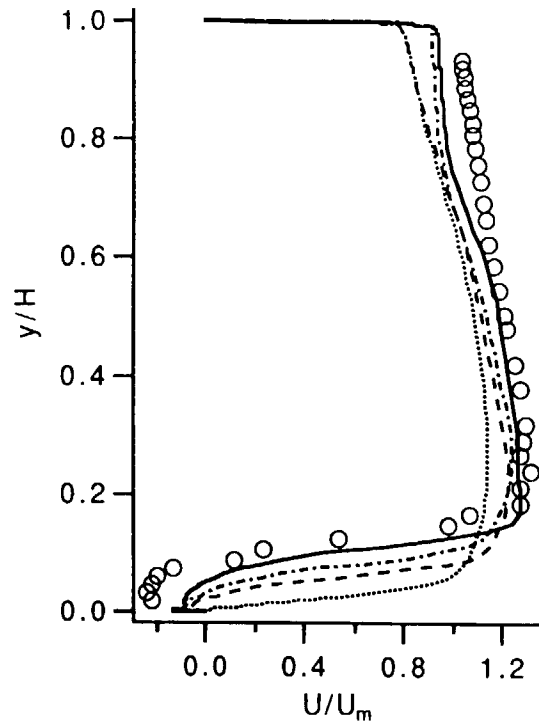




$\theta=30$  deg

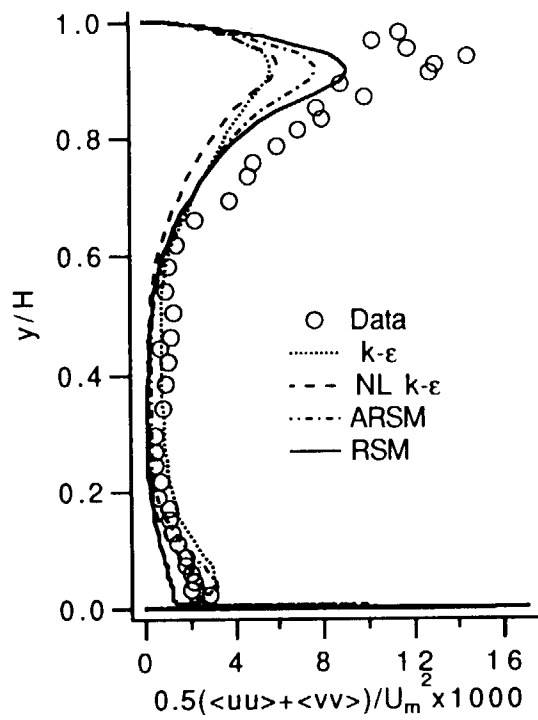


$\theta=90$  deg

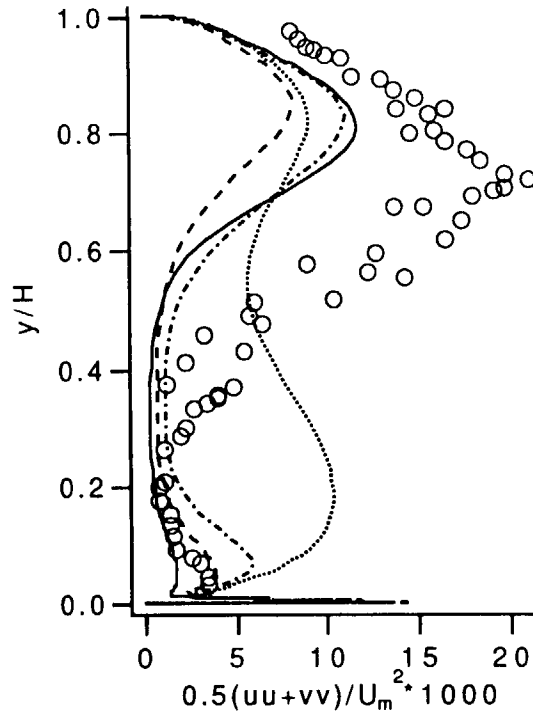


$\theta=180$  deg

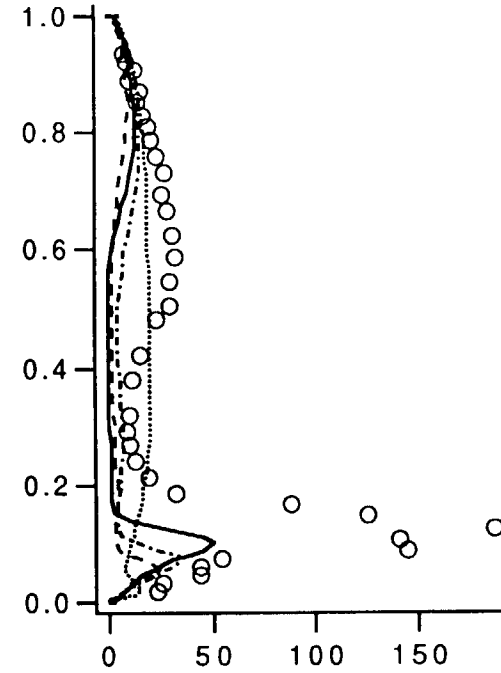
Fig. Variation of mean velocity profile of 180-deg duct flow



$\theta = 30$  deg



$\theta = 90$  deg



$\theta = 180$  deg

Fig. Variation of  $0.5(\langle uu \rangle + \langle vv \rangle)$  profile of 180-deg duct flow

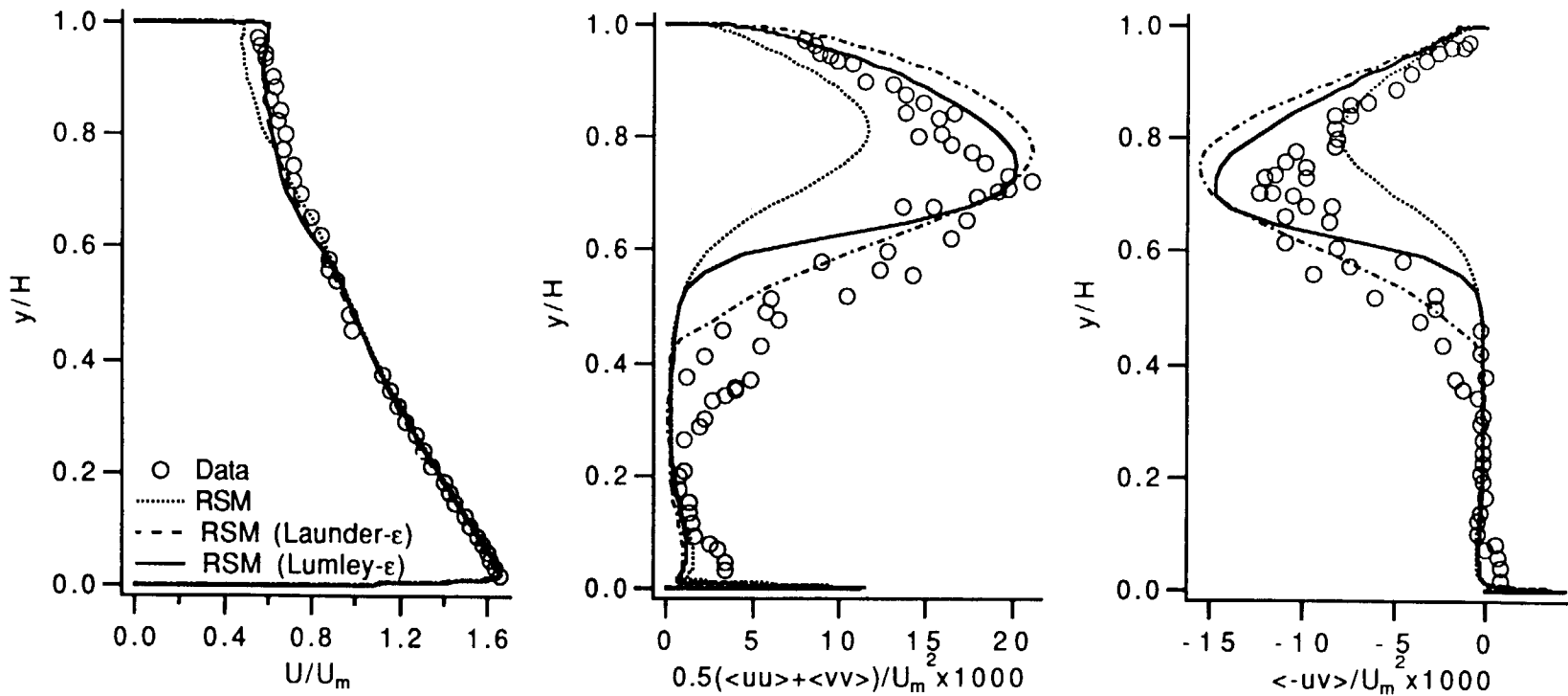
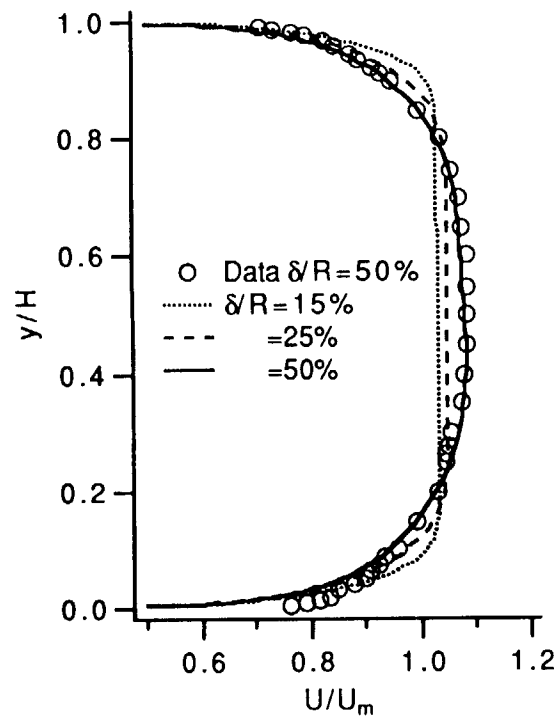
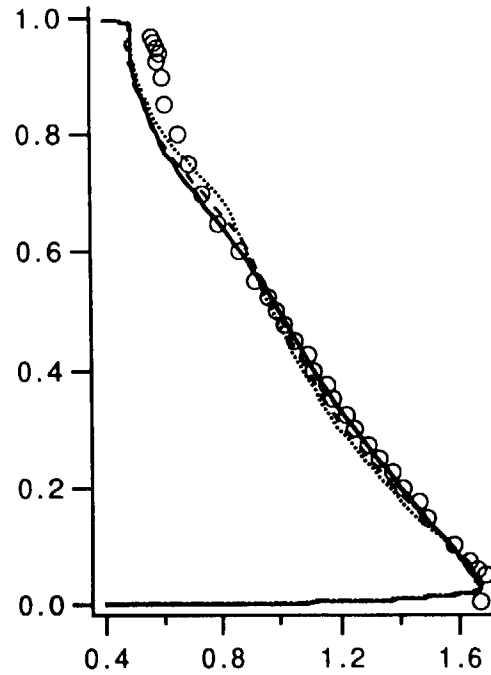


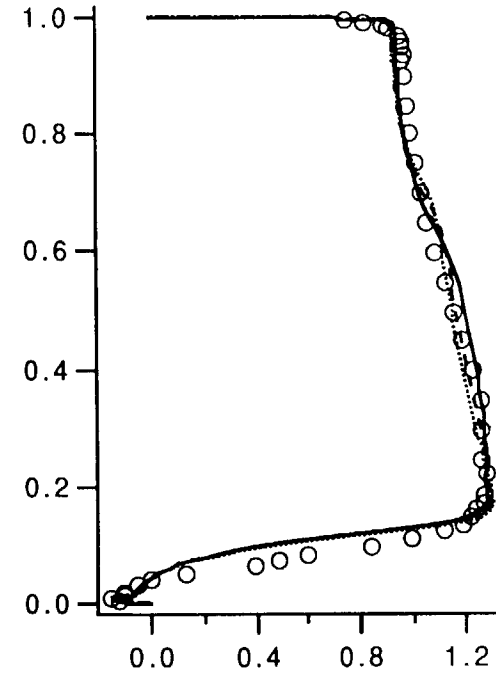
Fig. Profiles at  $\theta=90$  deg computed by RSM with modified  $\epsilon$ -eq.



$x = -1.73 H$



$\theta = 90 \text{ deg}$



$\theta = 180 \text{ deg}$

**Fig. Effects of  $\delta/R$  on mean velocity profile of 180-deg duct flow (Simulation by RSM model, data by Sandborn)**

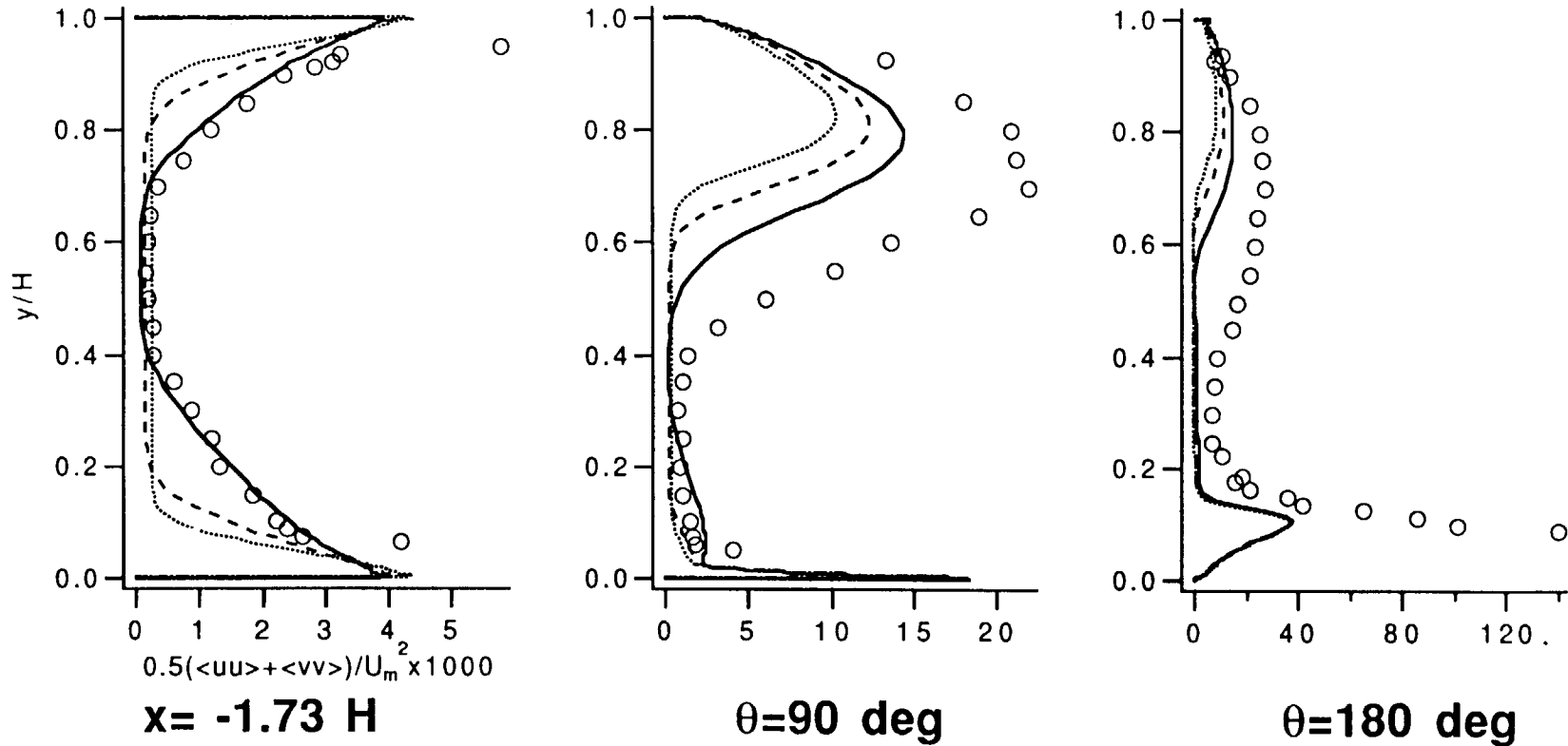


**Fig. Effects of  $\delta/R$  on turbulence energy profile of 180-deg duct flow (Simulation by RSM model, data by Sandborn)**

## Conclusions on Turbulence Modeling for Strongly Curved Flows

- RSM model provide best predictions for major features of the highly curved duct flows, including major attenuation of turbulence near the convex wall, strong enhancement of turbulence near the concave wall and the extensive separation downstream of the bend.

- Modeling convex curvature effects is different from modeling concave curvature effects, even qualitatively. RSM model is very successful in modeling convex curvature, while still underpredicts concave curvature effect.

- Turbulence damping due to convex curvature are also captured well by ARSM & Nonlinear  $k$ - $\varepsilon$  model. The isotropic  $k$ - $\varepsilon$  model fails to account for this effect and underpredicts the extent of separation.

- ARSM model is superior to nonlinear  $k$ - $\varepsilon$  model for the curved duct flows investigated. The nonlinear  $k$ - $\varepsilon$  model does not capture any turbulence enhancement in concave region.

- All the models provide too slow a recovery process from separation downstream of the bend, indicating defects in the modeling of turbulent diffusion as well as dissipation terms.

- Simulation studies & data indicate that the flow inside the bend is not sensitive to the upstream inflow conditions, different  $\delta/R$  leading to only minor variation in downstream velocity profiles.

449

- To capture concave curvature effect,  $\varepsilon$ -eq. must be modified:
  - Model of Launder et al. & Lumley provide some improvement.
  - Further improvement of  $\varepsilon$ -eq. is needed.

## Design Features of Penn State Turbine Nozzle

Hub tip ratio	0.7269
Tip radius	0.4582 m
Chord(tip)	0.1768 m
Spacing(tip)	0.1308 m
Turning angle	70 deg
Vane Re(outlet)	$(9-10) \times 10^5$
Exit Mach	0.27

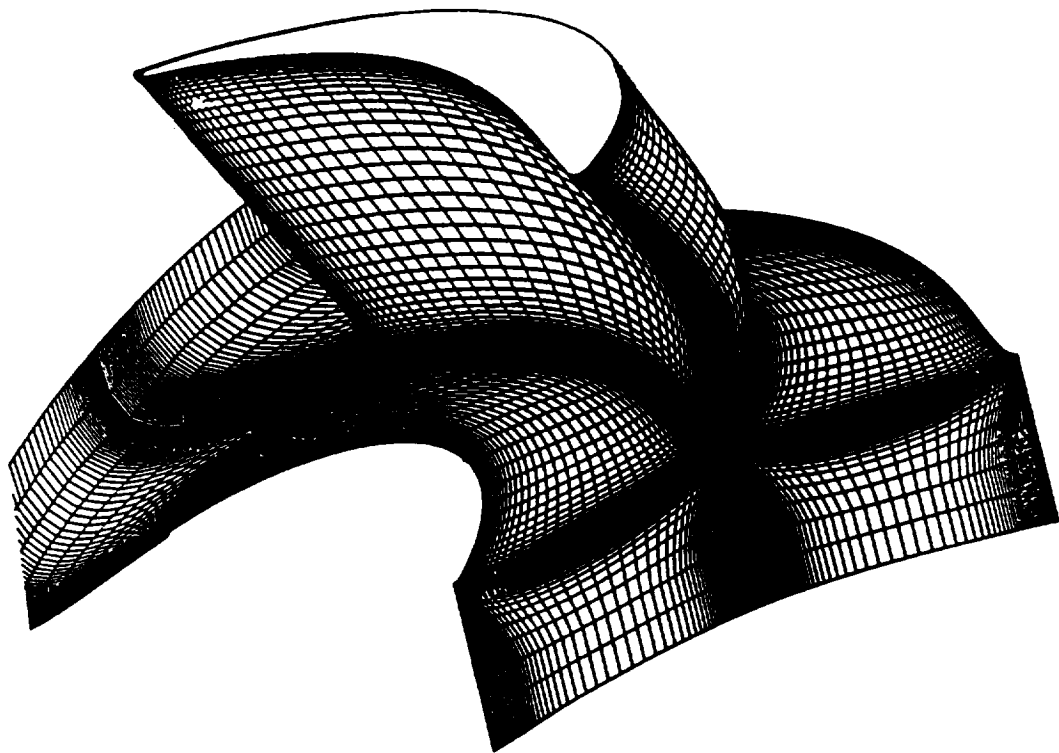


**Fig. 3a Computational grid for PSU turbine nozzle**



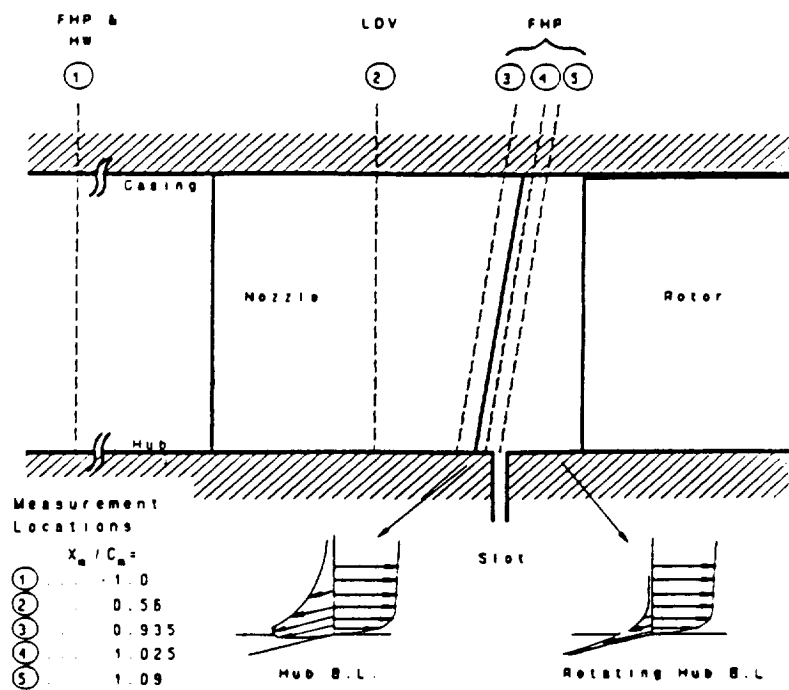


**Fig. 3b Measurement locations for the turbine nozzle  
(FHP: Five hole probe;  
LDV: Laser doppler velocimeter)**

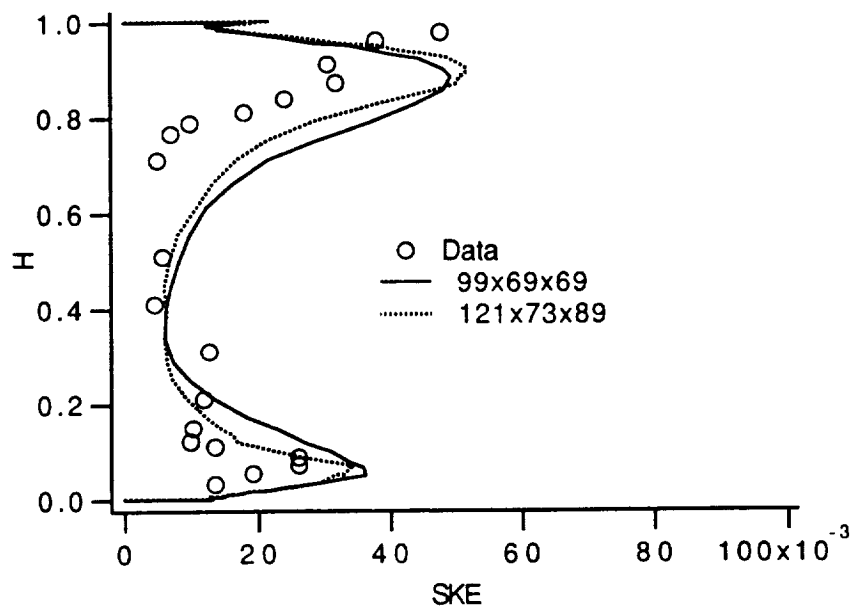
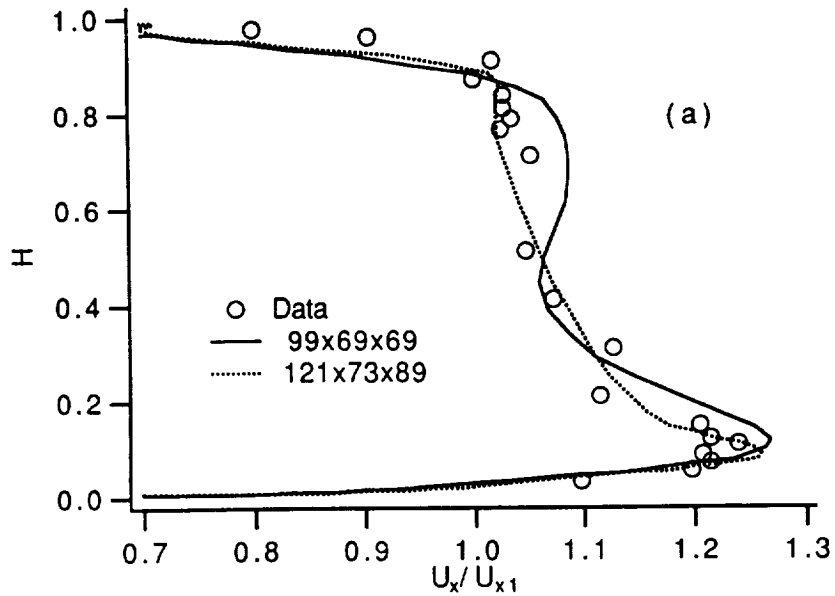
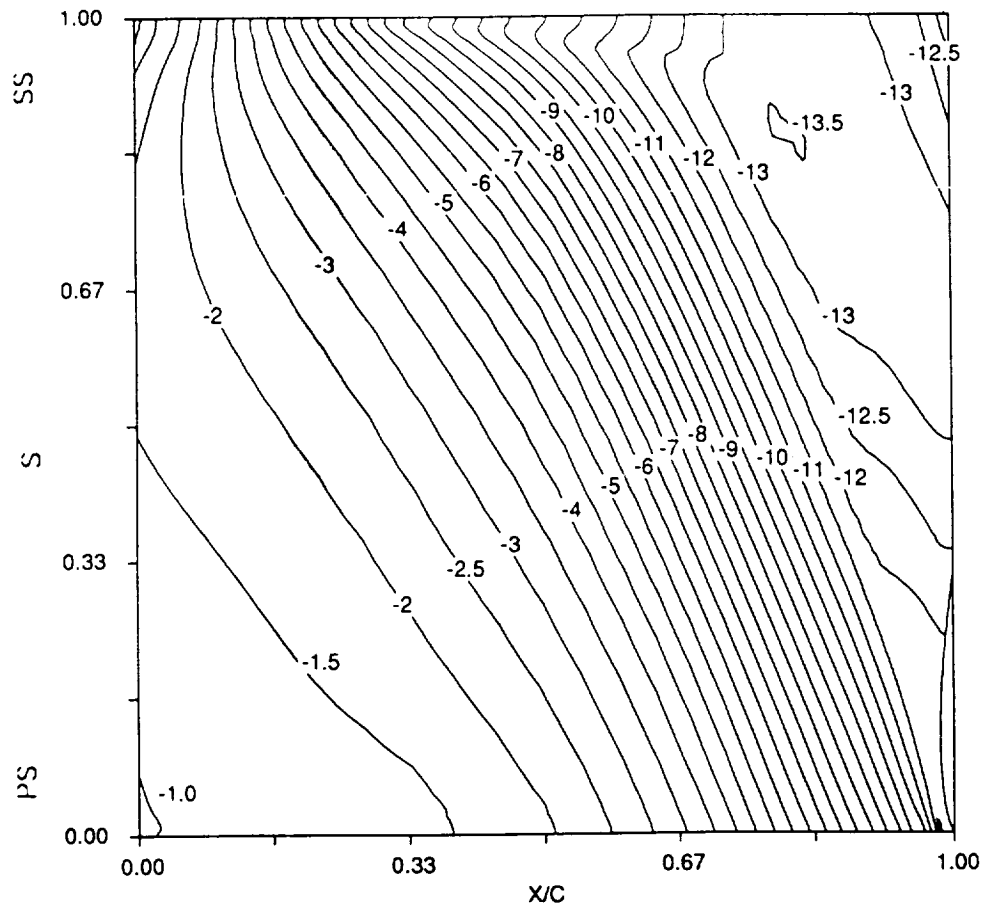
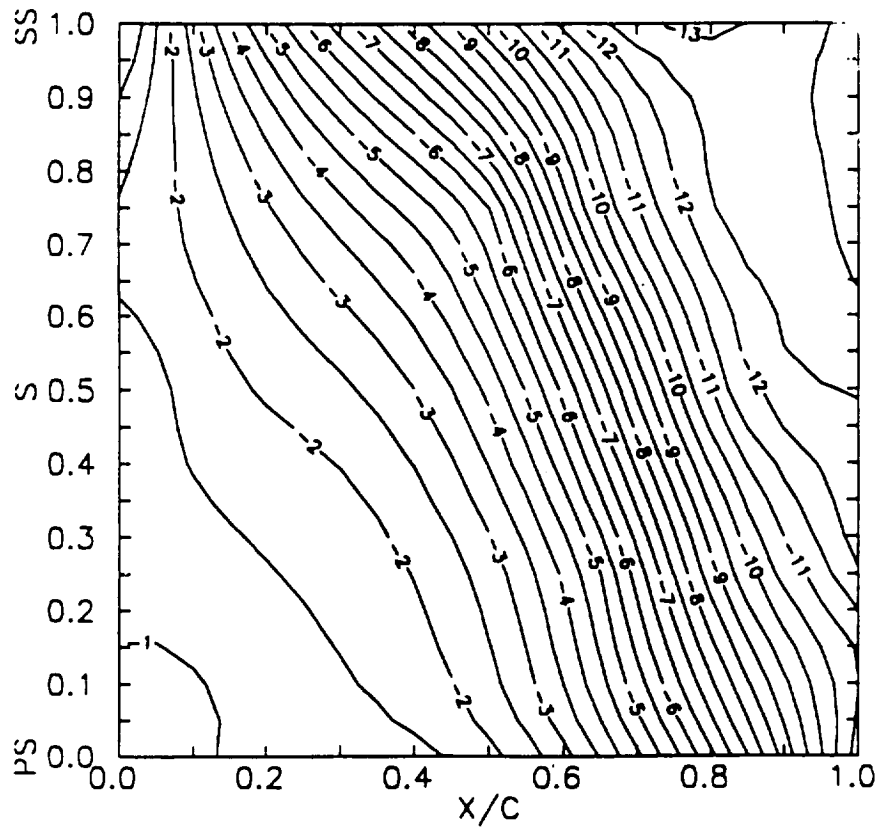


**Fig. Pitchwise-mass-averaged parameters (tangential velocity and secondary kinetic energy) predicted using 121x73x89 and 99x69x69 grids with k-ε model**



Computation by  $k-\epsilon$ /ARSM model



Measurement

**Fig. 7 Nozzle hub wall static pressure coeff. ( $C_p$ )**

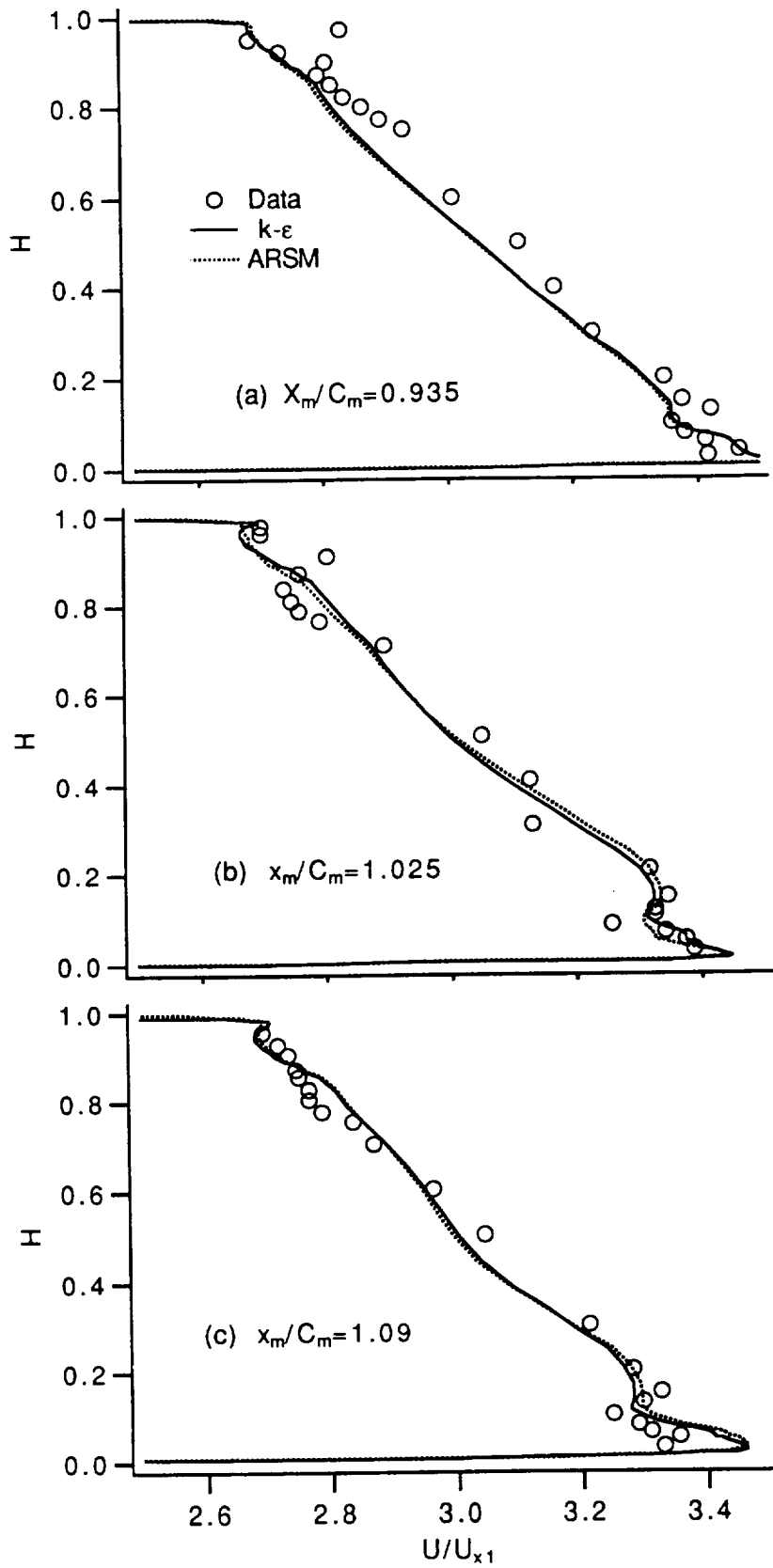


**Fig. Pitchwise-averaged total velocity profile**

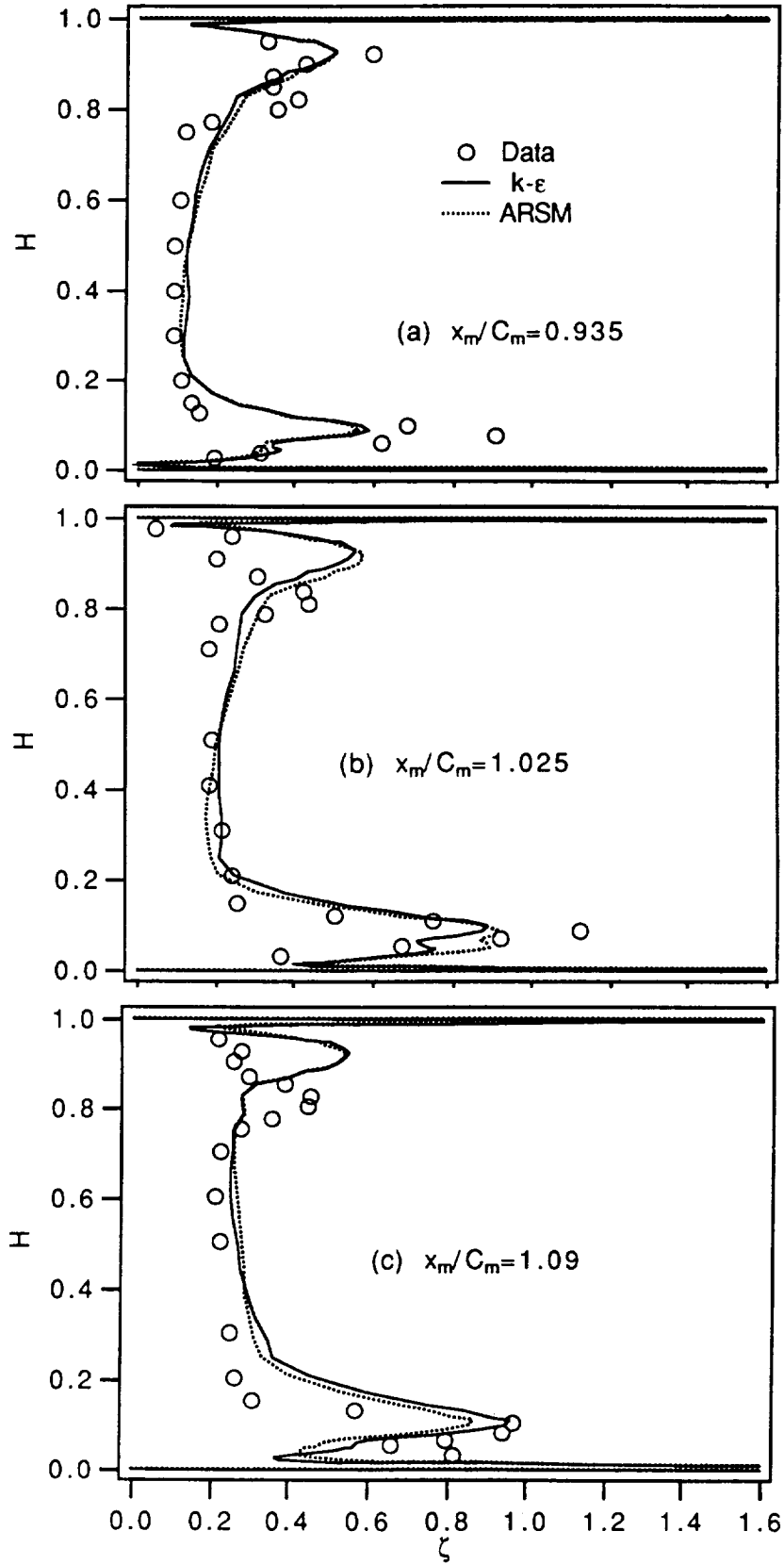


**Fig. Pitchwise-averaged total pressure loss coeff.**

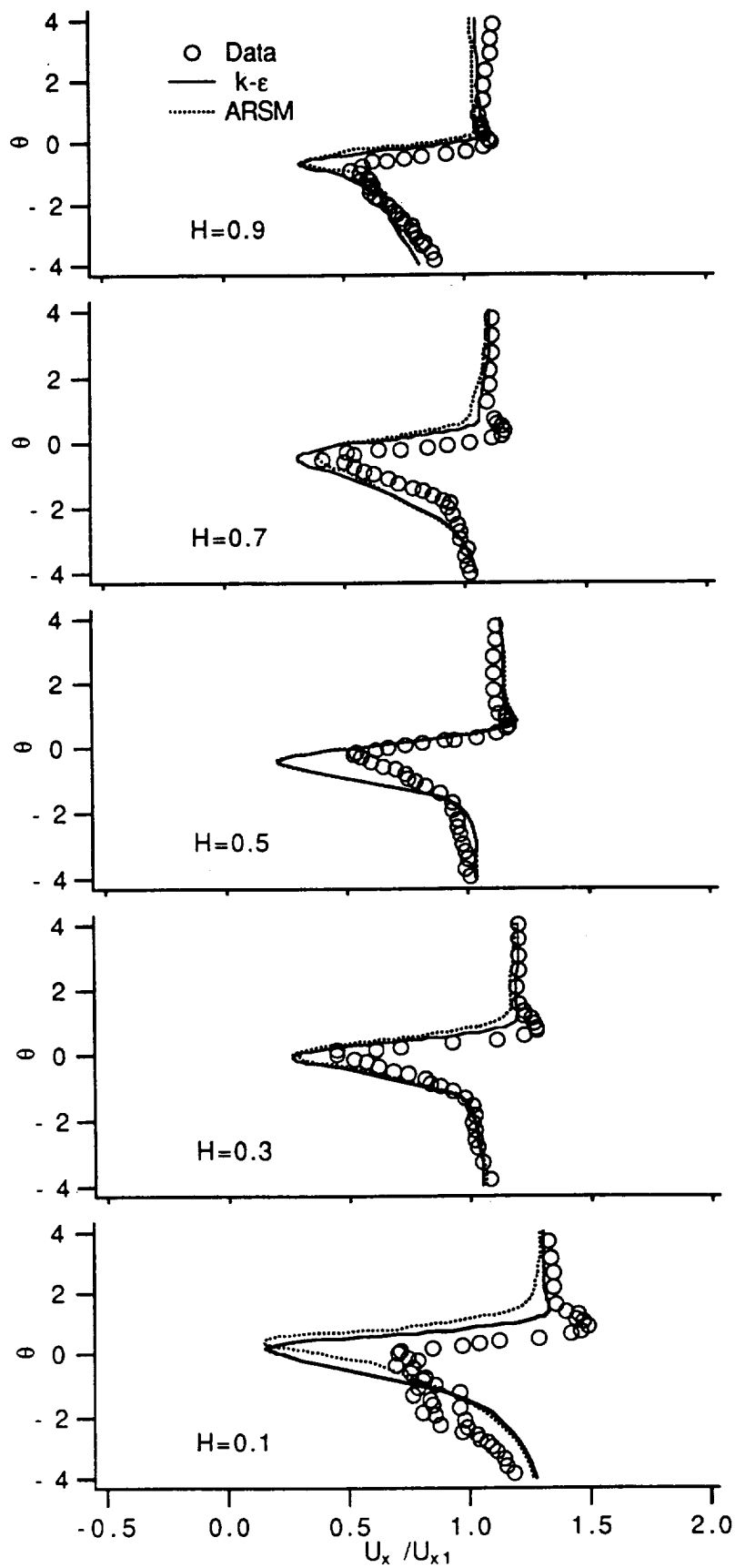


**Fig. 18b Axial velocity profile at  $x_m/C_m=1.025$**

## Conclusions

- Most features of the vortex-dominated endwall flow in the annular turbine nozzle have been captured accurately by the 3-D Navier-Stokes prediction. The passage-averaged properties, particularly the yaw angle and velocity profiles, are captured very well by the present numerical computation.

- The predictions by the anisotropic ARSM model are close to those by the isotropic  $k$ - $\epsilon$  model for the mean flow properties, although slight improvement in the prediction of secondary flow (e.g., the secondary kinetic energy) has been obtained by the ARSM model.

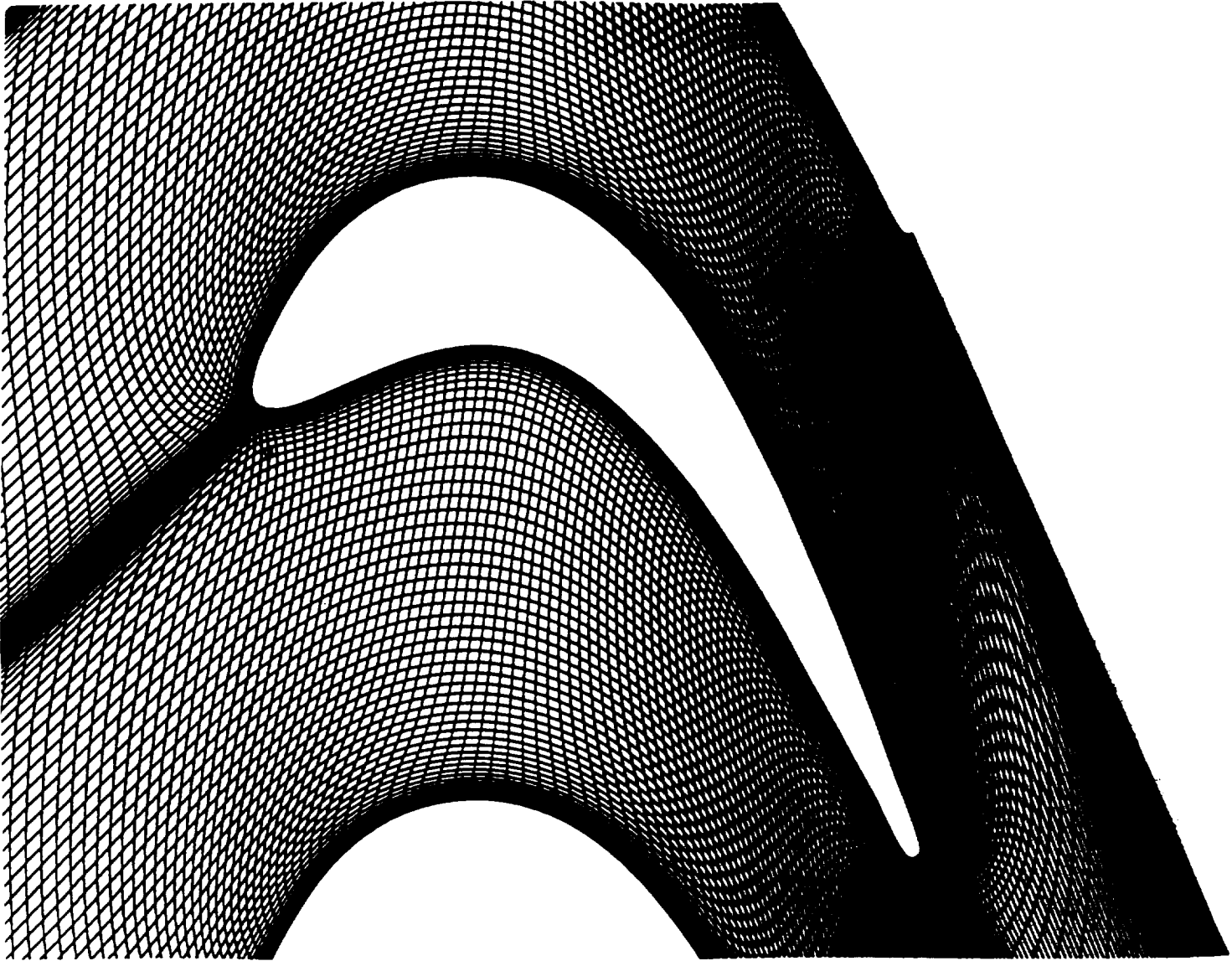
- The turbine nozzle secondary flows are primarily driven by pressure gradients. The anisotropy of turbulence becomes important when the secondary flow rolls up into a distinct vortex. Its dissipation and diffusion may only be captured by the ARSM and other anisotropic turbulence models.

• The wake profiles inside the endwall boundary layers are predicted better than those near the mid-span. The width and depth of the wake at the mid-span are overpredicted due to a premature transition predicted by the  $k-\varepsilon$  model on the blade suction surface in the presence of low freestream turbulence. The discrepancy in the wake profile are also due to the downstream rotor influence.



## PSU Rotor (midspan)

- Axial chord = 9.114 cm
- True chord = 11.13 cm
- Flow turning angle = 110 deg
- Re (exit) =  $5.7 \times 10^5$
- Mach (exit) = 0.27



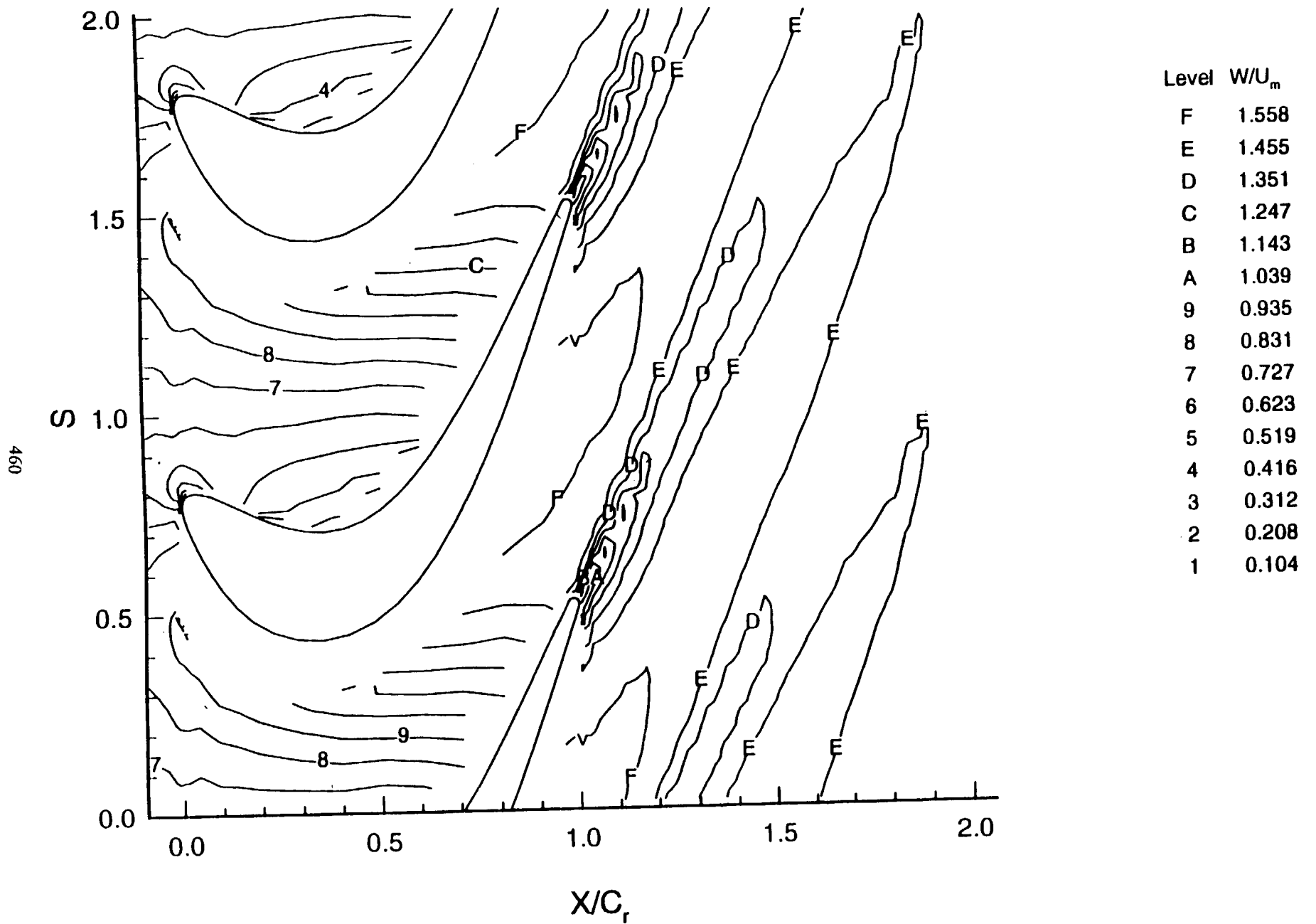


**Fig. Total velocity contour of PSU rotor midspan flowfield (Measurement at Penn State)**

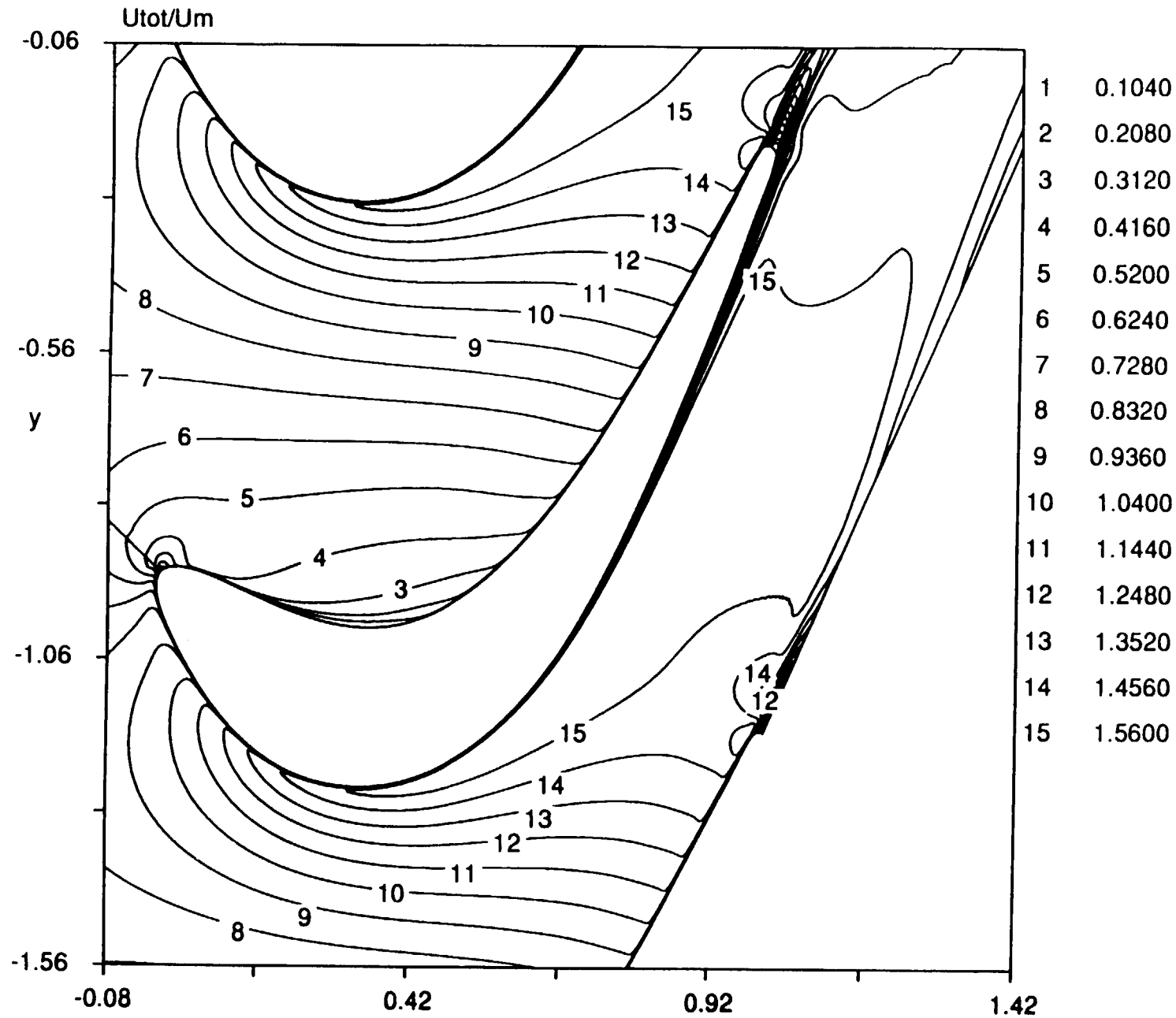
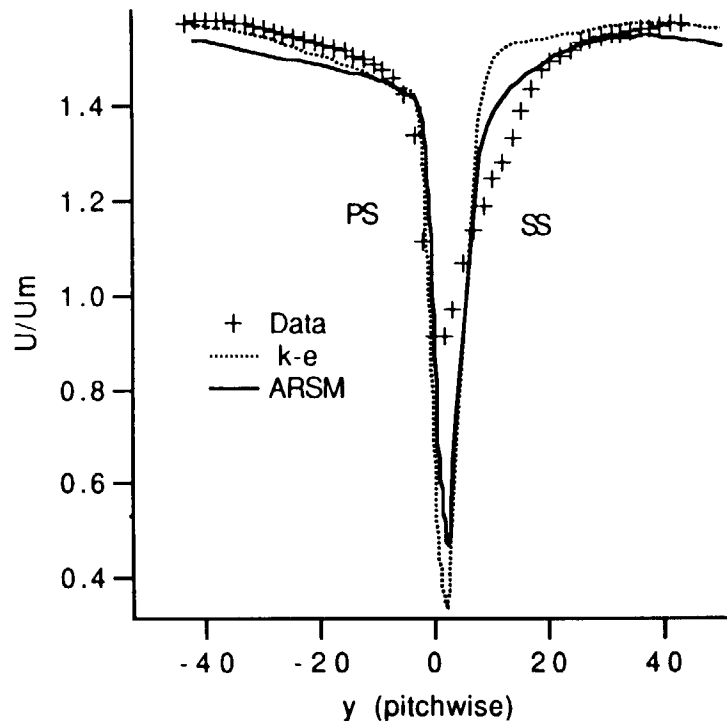
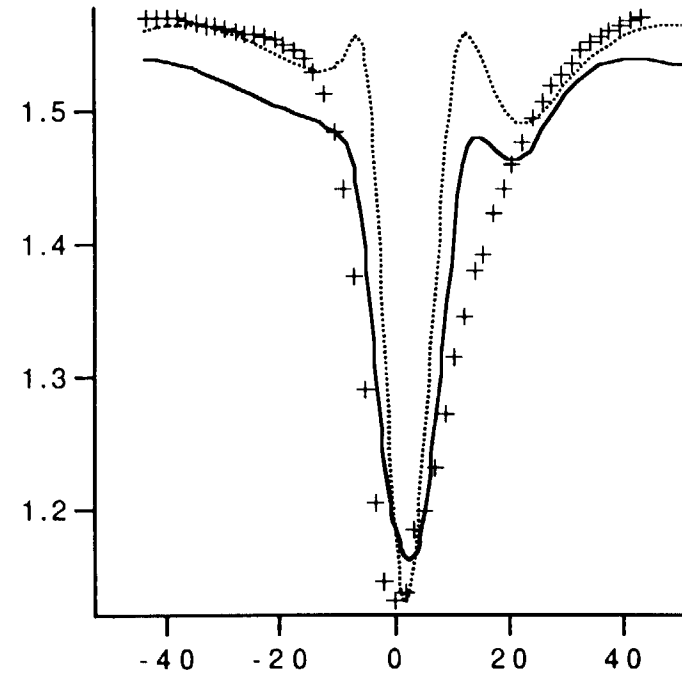


**Fig. Total velocity contour of PSU rotor midspan flowfield (computation with  $k-\epsilon$ /ARSM model)**



$x/C=102\%$

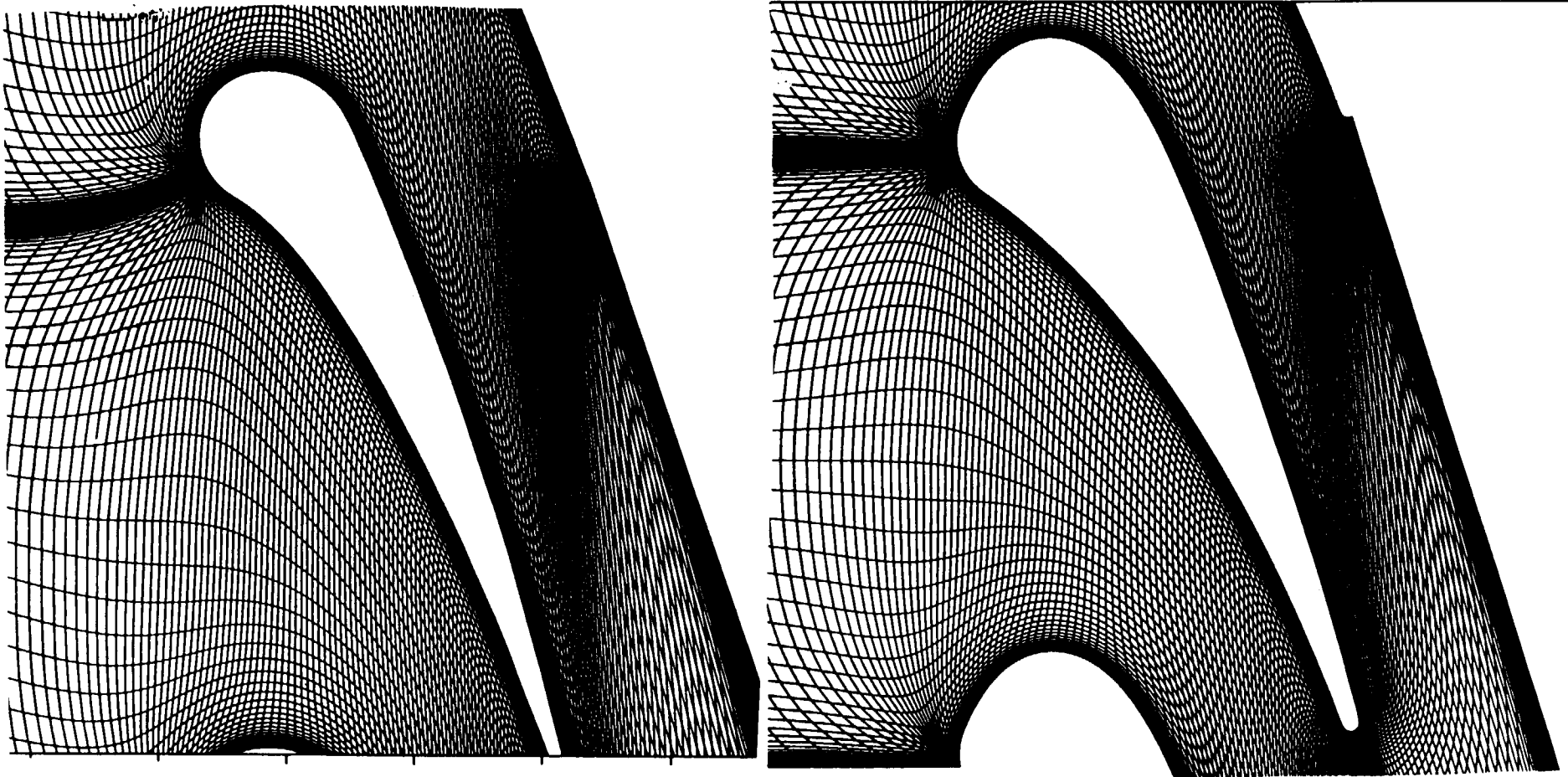


$x/C=112\%$

**Fig. Wake profile at midspan for PSU rotor flow**

Cascade geometries of Mark II and C3X:

	Mark II	C3X
Stagger angle (deg)	63.69	59.89
Air exit angle (deg)	70.96	72.38
Pitch (cm)	12.97	11.77
True chord (cm)	13.62	14.49



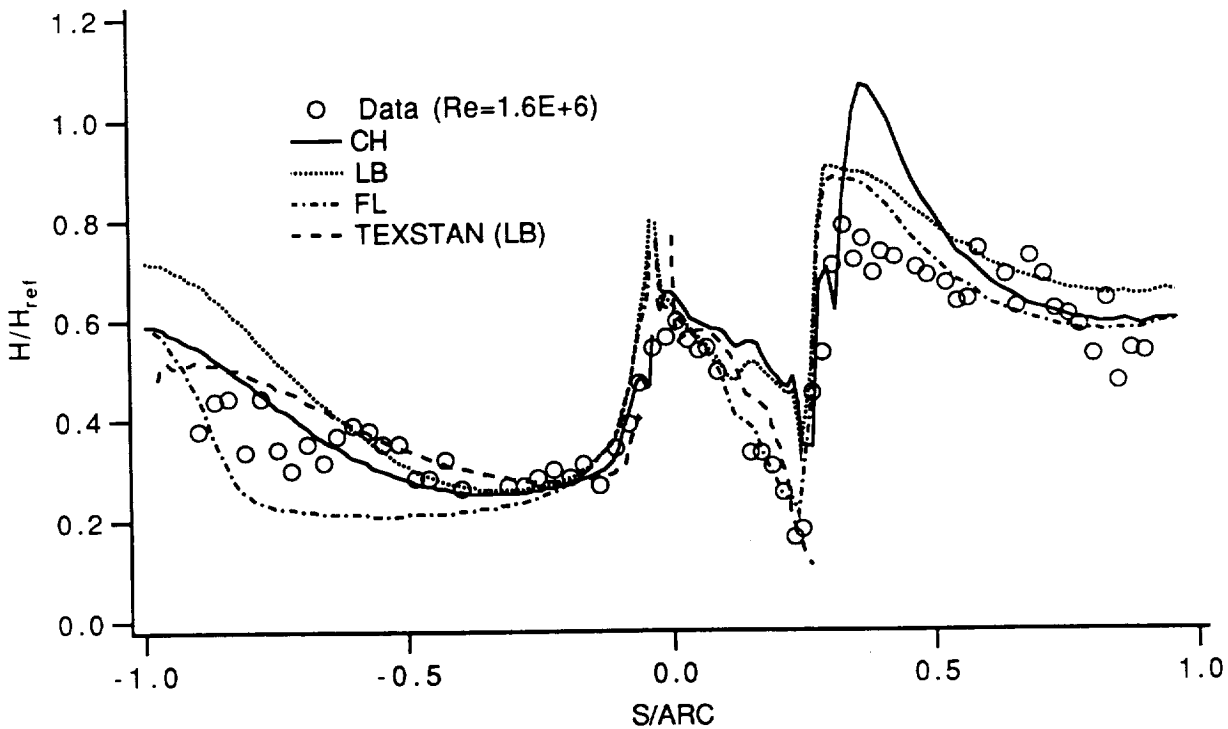


**Fig. 3(a) Heat transfer ( $H/H_{ref}$ ) prediction for case Mark15 ( $M_{is2}=0.90$ ,  $Re_{is2}=1.6 \cdot 10^6$ ,  $Tu_{\infty}=8.3\%$ )**

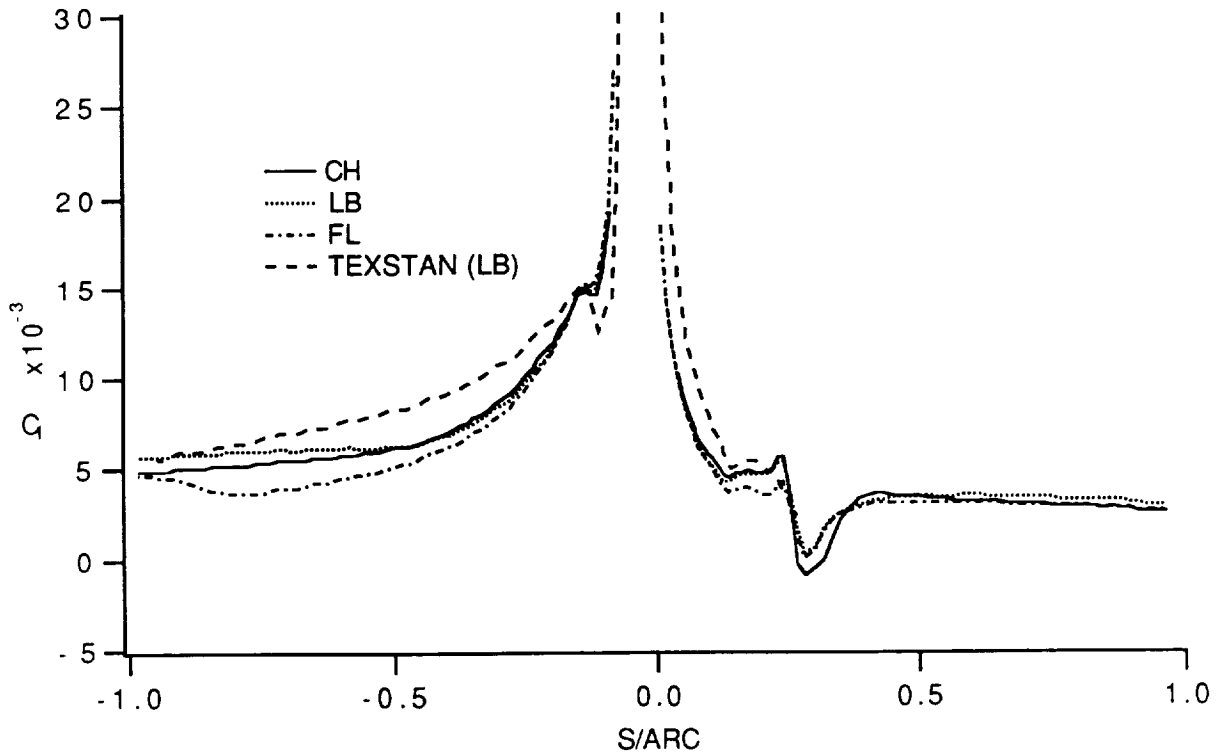


**Fig. 3 (b) Skin friction ( $C_f$ ) prediction for above case**

**Analysis of Heat Transfer for Mark II & C3X Turbine Nozzle Guide Vanes**  
with conditions ( $Re$ ,  $Tu$ ,  $T0$ ,  $Tw$ ) close to real engine conds.

- **Preds. with engr. accuracy obtained by CH, LB, FL k- $\epsilon$  models**
  - **LB prediction appears to be the best**
  - **CH performs well in fully turbulent region, but tends to smear out transition process, also not good for separation-induced transition**
  - **FL yield delayed transitions for accelerating turbine flows**
- **Separated-flow transition lead to much sharper increase of heat transfer than the nominal by-pass transition**
- **With minimum smoothing and good LRN k- $\epsilon$  model, 2-D N-S method provide good pred. of blade boundary layer development, transition & heat transfer under diff.  $Re$ ,  $Tu$ , etc.**

## Future Efforts

- **Turbulence modeling:**
  - Investigation of combined effects of curvature & rotation on turbulent flowfield in 3-D rotor flows
  - Modeling the source term in  $\varepsilon$ -equation to capture strong concave curvature; couple this with RSM
  - Modeling the  $\varepsilon$ -eq. & turbulent diffusion to improve the prediction of recovery process after re-attachment
- **Code Development:**
  - Multigrid solution of Reynolds stress transport equations
  - Development & implementation of full 3-D non-reflecting B.C.
- **Validation & Simulation:**
  - Modeling strong concave curved TBL & duct flows
  - Navier-Stokes simulation of rotor flow with non-reflecting boundary conditions & advanced turbulence models